An estimate of orange roughy, *Hoplostethus atlanticus*, biomass using the daily fecundity reduction method

John R. Zeldis*
R. I. Chris Francis
Malcolm R. Clark
Jonathan K. V. Ingerson
Paul J. Grimes
Marianne Vignaux

National Institute of Water and Atmospheric Research (NIWA)
P.O. Box 14-901, Kilbirnie, Wellington, New Zealand

*E-mail address: j.zeldis@niwa.cri.nz

Abstract.—The recruited biomass of orange roughy, *Hoplostethus atlanticus*, was estimated for the New Zealand mid-east coast orange roughy stock with the daily fecundity reduction method (DFRM). These fish migrate to Ritchie Bank and spawn between 850 and 900 m for about one month in winter. The biomass of spawning females was estimated by dividing mean daily planktonic egg production, N_0 (eggs/day), by mean daily fecundity, D (eggs/kg per day). The stock biomass was then estimated by multiplying the spawning female biomass by the ratio of all recruited fish to females that would spawn that year, estimated with a wide-area trawl survey made over the stock area two months before the spawning season.

The mean daily planktonic egg production was sampled near the peak of the spawning season, by using a stratified-random plankton survey. Eggs were staged and aged after accounting for their thermal history as they ascended the water column. Because young eggs were damaged by the net and older eggs were affected by advection out of the plankton survey area, relatively few egg stages were available for estimating N_0 (10.9×10^9 eggs/day), and the estimate was somewhat imprecise (CV=0.46). Mean daily fecundity (787 eggs/(kg × day), CV=0.11) was estimated from the daily rate of decline in population fecundity per mature female weight (R_i). Fecundity per female weight was estimated from a trawl survey made in the spawning area during the spawning season and was calculated as the mature eggs/kg of active spawners multiplied by the proportion of active spawners in each trawl. Spawning female biomass was 14,000 t (CV=0.50), and stock biomass was 26,000 t (CV=0.50). Mean daily fecundity was probably under-estimated because spent fish appeared to migrate from the spawning area during the fecundity reduction measurement period and reduce stock biomass to about 18,200 t. The DFRM biomass estimate was of central importance in the introduction of greatly reduced total allowable catch levels in this fishery.

Manuscript accepted 26 February 1997.
Fishery Bulletin 95:576–597(1997).

The orange roughy (*Hoplostethus atlanticus*, Trachichthyidae) fishery on Ritchie Bank on the eastern New Zealand continental slope (Fig. 1) was the second largest orange roughy fishery in New Zealand during the late 1980's and early 1990's, with a total allowable commercial catch (TACC) of about 10,000 metric tons (t) per year. Trends in catch per unit of effort (CPUE) indicated that the stock size was diminishing rapidly under this management regime, although the stock reduction analysis for the fishery did not estimate stock size precisely (Field et al.[1]). Experience with other major orange roughy fisheries in New Zealand (the "Box" fishery on northern Chatham Rise and the Challenger Plateau fishery [Fig. 1; Clark, 1995]) indicated that overfishing of the Ritchie Bank stock was likely because of low productivity. However, without adequate knowledge of stock size, it was difficult to set a TACC that would allow a sustainable fishery.

Zeldis (1993) concluded that both the annual egg-production method (AEPM; Saville, 1964; Picquelle and Megrey, 1993; Koslow et al., 1995) and the daily fecundity reduction method (DFRM; Lo et al., 1992; Lo et al., 1993) would be feasible for the estimation of absolute spawning biomass of orange roughy. A voyage was made to Ritchie Bank from early June to early July, 1993 (*Tangaroa* voyage TAN9306), with the intention of using both types of egg-production survey method. With the AEPM, annual egg production is the sum of daily planktonic egg production estimates made over the entire spawning season from separate subsurveys. Unfortunately, the voyage failed to sample annual egg production for two reasons. First, although the voyage was executed as a series of five subsurveys, two of the subsurveys were not completed because of ship and equipment breakdowns and because of a lack of time at the end of the voyage. Second, the voyage period ended before spawning had finished for the season, so that the annual egg production was not completely sampled.

[1] Field, K. D., R. I. C. C. Francis, and J. H. Annala. 1993. Assessment of the Cape Runaway to Banks Peninsula (ORH 2A, 2B, and 3A) orange roughy fishery for the 1993–94 fishing year. MAF Fisheries, Fisheries Assessment Research Document 93/8. NIWA, Greta Point, Wellington, New Zealand, 17 p.

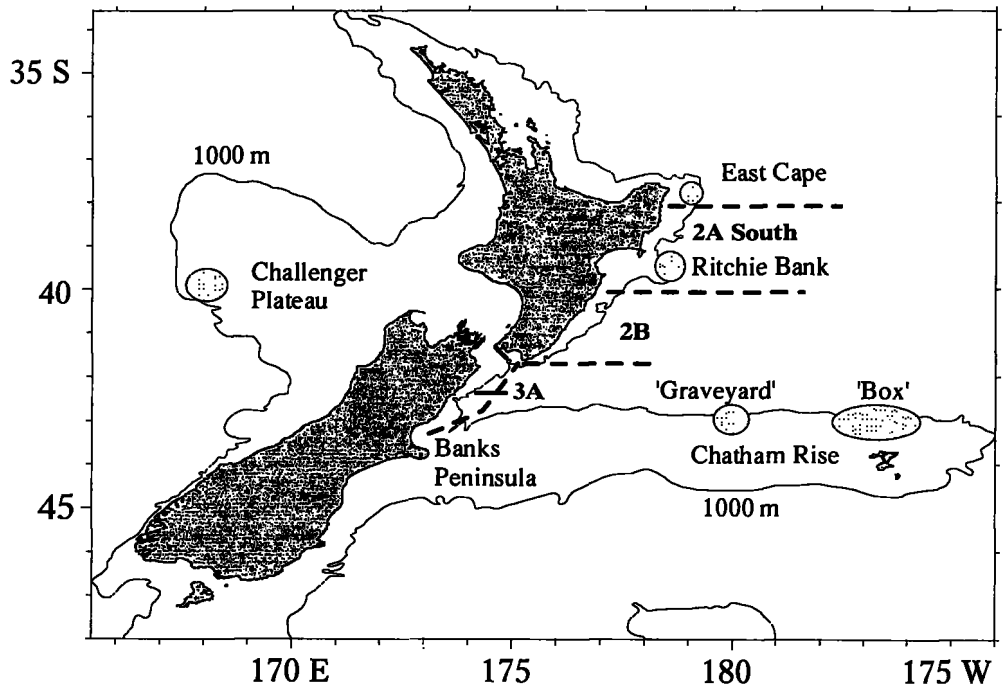

Figure 1

Map of New Zealand and location of spawning grounds (ovals) of orange roughy, *Hoplostethus atlanticus*. Also shown are the areas (2A, 3B, and 3A) of the east coast stock.

Unlike sampling for the AEPM, sampling for the DFRM did not need to cover the entire spawning season, allowing an estimate of spawning female biomass on Ritchie Bank to be produced from the portion of the voyage that did not suffer from ship and equipment breakdowns and that provided adequate data on planktonic egg production and fecundity. The DFRM was used to estimate the biomass of spawning females by dividing the daily planktonic egg production in the survey area (eggs/day) by the daily fecundity of females (eggs/(kg × day). The biomass of spawning females was scaled by the maturity ogive, sex ratio, and spawning proportion to estimate the recruited biomass (≥32 cm standard length) of orange roughy in the stock (where the stock is defined as those fish assumed to spawn on Ritchie Bank). The latter data were taken from a wide-area trawl survey in March–April 1993 (*Tangaroa* voyage TAN9303; Field et al.[2]), that covered the area inhabited by the stock (Banks Peninsula to East Cape, Fig. 1).

A necessary biological prerequisite for using the DFRM is that the target species has determinate annual fecundity (Hunter and Lo, 1993). This enables total seasonal fecundity to be determined before final maturation so that the fecundity reduction rate can be monitored through the spawning season (Lo et al., 1993). Orange roughy have determinate annual fecundity (Pankhurst et al., 1987; Bell et al., 1992; Zeldis, 1993). Application of egg production methods to orange roughy also is possible, but only if the age of planktonic eggs at morphological stage can be estimated. Ageing of eggs was achieved by developing a model for ageing the eggs as they traversed the thermal gradient in the water column (Zeldis et al., 1995) and by describing the morphological stages of the eggs (Grimes et al.[3]).

DFRM model

To calculate the biomass of Ritchie Bank spawning females, the daily planktonic egg production in the

[2] Field, K. D., R. I. C. C. Francis, J. R. Zeldis, and J. H. Annala. 1994. Assessment of the Cape Runaway to Banks Peninsula (ORH 2A, 2B, and 3A) orange roughy fishery for the 1994–95 fishing year. MAF Fisheries, Fisheries Assessment Research Document 94/20. NIWA, Greta Point, Wellington, New Zealand, 24 p.

[3] Grimes, P. J., A. C. Hart, and J. R. Zeldis. 1997. Embryology and early larval development of orange roughy (*Hoplostethus atlanticus* Collett). Unpubl. data.

survey area was divided by the daily fecundity/kg of the females:

$$B_{spf} = N_0/(1{,}000D),$$

where B_{spf} = biomass of spawning females (tons);
N_0 = daily egg production, (eggs/day);
D = mean daily fecundity (eggs/(kg × day)) for mature fish; and the factor 1,000 converts kg to tons.

The recruited biomass, B_{rec} (defined as the biomass of fish of length ≥32 cm) was calculated from the biomass of Ritchie Bank spawning females, B_{spf}, as

$$B_{rec} = B_{spf}S,$$

where the scalar (S) was an estimate of the ratio B_{rec}/B_{spf}. This ratio allows for recruited females that did not spawn, females that did spawn but were <32 cm, as well as the sex ratio.

To estimate the parameters of the above biomass model, the data analysis deals with three distinct data sets:

- daily planktonic egg production;
- daily fecundity per female weight; and
- proportions spawning, recruited, and female.

Daily planktonic egg production

Survey design The timing of plankton sampling coincided with the period when orange roughy females on the Ritchie Bank were in late maturation or spawning stages (mid-June to the end of the first week of July; Pankhurst, 1988). The location of plankton sampling was determined from research trawl catch rates (Fincham et al.[4]), which showed adult biomass to be highly aggregated on Ritchie Hill[5] (Fig. 2, A and B) at the northern end of Ritchie Bank. Ritchie Hill catch rates accounted for 84% of the relative orange roughy biomass over the Ritchie Bank survey area in July 1986 (Fincham et al.[4]). In plankton sampling during the spawning season on Ritchie Bank in early July 1986,[6] orange roughy eggs were caught only at stations near Ritchie Hill, and samples taken ≥20 km away contained no eggs, indicating that eggs were aggregated near the spawners (Zeldis, 1993) and that plankton sampling would need to be highly concentrated near Ritchie Hill.

During their first 36 hours of development, orange roughy eggs ascend the water column at 300–350 m/day from a spawning depth of about 850 m (Zeldis et al., 1995). Geostrophic currents over Ritchie Bank during July 1986[6] were to the south and averaged about 12 cm/sec between 700 m and 250 m; these currents would displace these eggs at least 15.5 km to the south of Ritchie Hill by the time the eggs had reached 36 h of development (this is a minimum estimate because there was probably some residual flow at the postulated level of no motion at 700 m). Considering that drift would probably vary in direction and speed but would lie predominantly along isobaths, we designed the survey area with eight strata, elongated alongshore and arranged symmetrically around a central stratum centred over the top of Ritchie Hill (Fig. 2B). This central stratum (10.0 × 7.6 km) was about the size of the area of high fish density observed during a trawl survey done in the area in June–July 1987 (Grimes[7]). The middle layer of four strata surrounding the central stratum had outer boundaries of 18.5 ×13.7 km. These dimensions were chosen to approximate the distance at which catch rates of 1-day-old orange roughy eggs on the St. Helen's seamount in eastern Tasmania were reduced to half (9.3 km from the spawners [Koslow[8]]). The outer layer of four strata had an outer boundary 40.0 × 30.0 km long, to allow for maximal drift of 36-h-old eggs.

The St. Helen's data were used to estimate optimal allocation of stations to Ritchie Hill strata. The St. Helen's data were collected over an entire spawning season, in six separate subsurveys, each of which had two spatial strata. The counts in each St. Helen's subsurvey and stratum were standardized such that their means equalled the mean across all of the subsurveys for each stratum. This procedure removed the within-season variation in mean egg density in each stratum. These standardized data were then laid over the Ritchie Bank stratum layers (central, middle, and outer), and mean egg densities (M_j) were estimated for each stratum layer, j. To allocate sta-

[4] Fincham, D. J., D. A. Banks, and P. J. McMillan. 1987. Orange roughy trawl survey, Tolaga Bay to Cape Turnagain, 14 June to 11 July 1976: cruise report. Fisheries Research Division Internal Report 60. NIWA, Greta Point, Wellington, New Zealand, 38 p.

[5] The names "Ritchie Bank," "Ritchie Hill," and "North Hill" used in this paper refer to the features called "Ritchie Ridge," "Calyptogena Bank," and "Pantin Bank," respectively, in the following: Arron, E. S., and K. B. Lewis. 1992. Mahia, 2nd ed. N.Z. Oceanogr. Inst. Chart, Coastal Series, 1:200,000. NIWA Greta Point, Wellington, New Zealand.

[6] Zeldis, J. R. 1986. Cruise report J08/86 (second half). MAF Fisheries unpublished cruise report held in NIWA Library, Greta Point, Wellington, New Zealand, 7 p.

[7] Grimes, P. 1987. NIWA, P.O. Box, 14-901, Kilbirnie, Wellington, New Zealand. Unpubl. data.

[8] Koslow, T. 1992. CSIRO Division of Fisheries, GPO Box 1538, Hobart, Tasmania 7001, Australia. Personal commun.

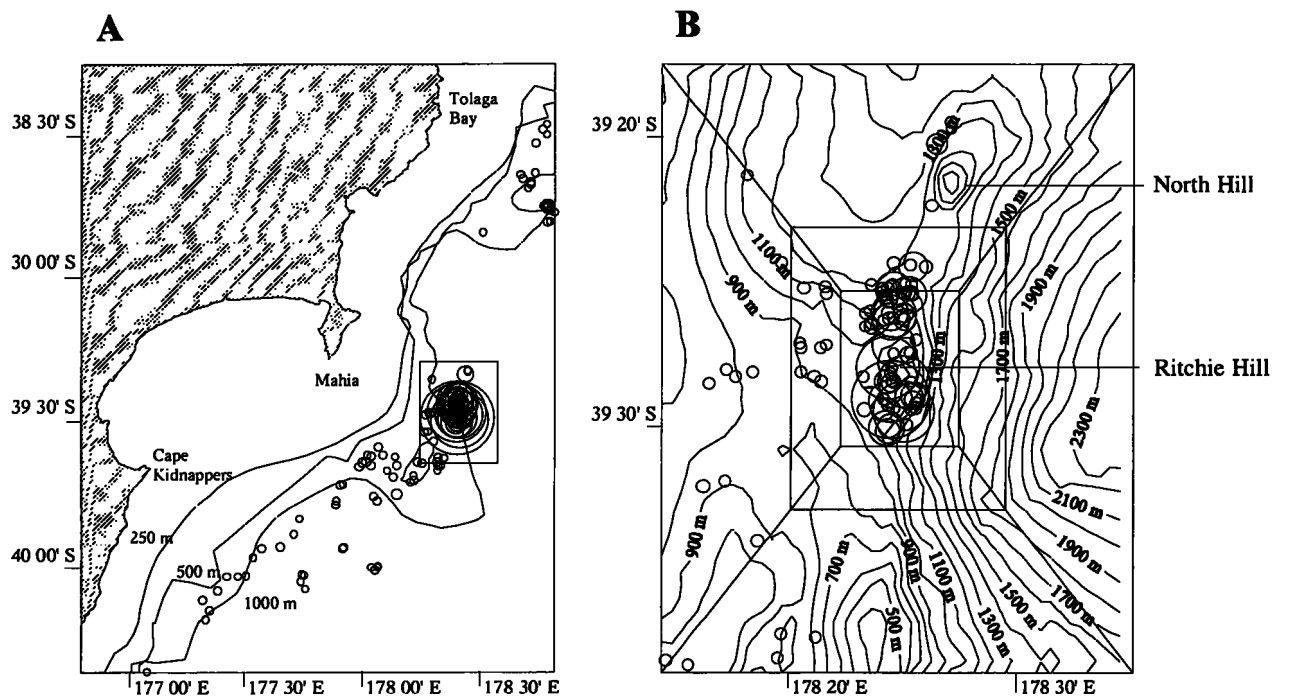

Figure 2

Bathymetry, station positions, and adult catch rates from trawl surveys in July 1986 (see Footnote 4 in the text) and June–July 1987 (Footnote 7 in the text) (**A**) over the wider east coast area, and (**B**) in the Ritchie Hill–North Hill area (area within rectangle in A). In A and B, circle areas are proportional to catch rate (tons/km towed), with largest circle = 860 tons. Strata for the egg production plankton survey are shown in B.

tions optimally in a survey of size N stations, n_j stations were allocated to each stratum layer such that

$$n_j \propto A_j M_j$$

and

$$\sum_j n_j = N,$$

where A_j = the area of each stratum layer.

Allocation was done in proportion to the strata means (M_j) because they were highly correlated with the strata standard deviations and were probably estimated more reliably than the standard deviations (Francis, 1984). To estimate values of N that would yield a desired coefficient of variation for egg abundance estimates, the standardized counts in each stratum layer were randomly sampled with replacement (bootstrapped) to estimate M_j, where the number of samples taken from each stratum was n_j. The survey mean egg abundance combined across all strata, E, was estimated as

$$E = \sum_j M_j A_j.$$

This procedure was repeated 500 times and the mean of the 500 survey estimates was taken as the egg abundance estimate. The standard deviation of the 500 estimates divided by the mean was taken as the coefficient of variation of the egg abundance estimate.

This analysis suggested that the optimal allocation would have stations allocated to the central, middle, and outer strata in ratios of 1.5:0.38:0.25, respectively. It also suggested that 400 stations would provide adequate precision (CV=0.15) in the egg abundance estimate. Therefore, for the AEPM design, five 80-station subsurveys were planned with stations allocated to strata in the above ratios.

Using simulations, we found that by occupying stations within each stratum in an order which minimized steaming distance between stations, before moving to a new, randomly chosen stratum, about 50% less steaming time would be involved than by occupying stations in completely random sequence in each subsurvey. This procedure would be done, however, at the cost of variable (and possibly long) periods of no coverage of each stratum between subsurveys and could be a serious drawback if spawning intensity varies significantly and rapidly (over a few days) during

the spawning season, especially for coverage of the central stratum. To counteract this, the stations in the central stratum were divided randomly between two time strata to reduce the time between occupation of this high-density stratum between subsurveys.

In the DFRM analysis, the plankton samples used for the estimation of egg production were from two consecutive AEPM subsurveys that were occupied near the peak of the spawning season and that were not subject to "downtime" from ship and equipment failures. These two subsurveys had no time break between them and were treated as a single survey, in which the central stratum was occupied four times and each of the surrounding strata was occupied twice. The plankton sampling in the entire survey was done from 14 June to 7 July, and the two subsurveys used in the DFRM analysis were done from 28 June to 6 July (subsurveys 3 and 4).

Egg sampling and staging, count standardization, and production estimation The plankton net used in sampling had a cylinder-cone design with 900-μm mesh, a mouth area of 2 m^2, and was fitted to a 125-kg flat-steel ring. It was designed to be efficient, with the ratio of the open area in the mesh to mouth area being >5:1 (Tranter and Smith, 1968). The net was deployed from a starboard crane while the ship was stationary (i.e. not under power) and its starboard side faced the wind. The winch had dynamic tensioning, to minimize surging of the net as a result of the rolling motion of the ship. Tow depths were within 30 m of the bottom to the surface if the bottom was less than 950 m and from 850 m if the bottom was deeper than 950 m. A conductivity-temperature-depth (CTD) probe or a net sonde within the mouth of the net was used to measure net depth. Warp payout was measured with winch instrumentation. Warp payout and recovery rates were 1 m/sec, also measured with winch instrumentation.

Eggs were staged (Grimes et al.[3]) on board, prior to preservation, and generally within 0.5 h of landing the net, except for two samples with many eggs. For these, staging was done partly on board and partly in the laboratory on 4% formaldehyde-preserved eggs. All eggs ≤ stage 7 (32-cell) were grouped, because it was not possible to identify with confidence the stages from germinal disk through 32 cells within the plankton samples because most of these younger eggs were damaged (76% of the 8,293 eggs ≤ stage 7), which caused the cell walls of the embryos to rupture, the cells to fuse, and the perivitelline space to collapse. Justification for assuming that the damaged eggs were all ≤ stage 7 are given in Zeldis et al. (1995) and Grimes et al.[3]

The standardization from egg count to egg density (eggs/m^2) was based on the formula *density* = *count* × *correction factor*, where the correction factor takes into account the mouth area of the net and the volume of water filtered by it. With a vertical haul, the correction factor is 0.5 (because the net mouth area=2 m^2). However, because the vessel almost always drifted (owing to wind and current) during shooting and hauling, hauls were not vertical and therefore the correction factors were almost always <0.5. Distance towed was not estimated by using flowmeters because flowmeters were found to record spurious revolutions during the deployment (descent) phases of tows in subsequent tests (Grimes[9]). Instead, to calculate the volume of water filtered by the net, it was necessary to use global positioning satellite (GPS) vessel positions, warp length, depth, and current velocities to infer the path of the net (which, because of the ship's drift, would be curved in the vertical dimension during hauling; Appendix 1).

With a curved net trajectory, there was a different correction factor for each combination of plankton tow and egg stage because the different egg stages occupied different depths as they ascended the water column and because the net sampled more water in layers of equal thickness in the upper water column than in the lower column. To calculate egg age and depth range (Table 1), data on egg development rate as a function of temperature, buoyancy by egg stage, and temperature as a function of depth were

[9] Grimes P. 1996. NIWA, P.O. Box 14-901, Kilbirnie, Wellington, New Zealand. Unpubl. data.

Table 1

Egg age (h) and depth (m) ranges used in calculating correction factors for count standardization for Ritchie Bank plankton samples. Egg stages are described in Grimes et al. (Footnote 3 in the text).

Stage	Min. age	Max. age	Max. depth	Min. depth
0	0.0	0.0	850	725
1	0.0	5.1	850	784
2	5.1	8.2	784	743
3	8.2	11.2	743	704
4	11.2	14.0	704	667
5	14.0	16.7	667	631
6	16.7	19.3	631	596
7	19.3	21.8	596	563
8	21.8	24.1	563	531
9	24.1	26.3	531	500
10	26.3	28.4	500	470
11	28.4	33.4	470	400
12	33.4	40.0	400	301
13	40.0	45.5	301	216
14	45.5	50.2	216	143
15	50.2	54.3	143	78

used with the methods of Zeldis et al. (1995) and the Ritchie Bank CTD temperature profiles described below. Ritchie Bank temperatures were within the range of those observed in Zeldis et al. (1995). Current velocities as a function of depth were calculated from geostrophic velocity profiles (Pond and Pickard, 1978) by using Guildline CTD profiles taken over Ritchie Bank. A reference depth of no motion at 1,000 m was assumed, and geostrophic velocities at 100 m were corrected to match the 100-m velocities measured by a buoy drogued to that depth. This buoy was deployed over Ritchie Hill on 28 June 1993, relocated 20 hours later, and subsequently lost.

Correction factors were to convert egg counts to densities were also calculated (assuming the trajectory of the net was straight) for comparison with those where a curved trajectory was assumed. For this, the volume filtered v (m^3) was estimated by using

$$v = 2\sqrt{p^2 + z^2},$$

where p = the distance the ship drifted from deployment to recovery of the net, determined with GPS;
z = the maximum depth of the net; and
factor 2 = the area (m^2) of the net mouth.

It was assumed that, at the start of hauling, the net was at the position of the vessel when deployment commenced, i.e. the net dropped vertically through the water during deployment.

Estimates of egg abundance by age group in the survey area (N_a) were calculated by multiplying the mean egg density at age in each stratum by stratum area and by summing across strata. In the case of the time strata in the center of the survey area, the egg abundances were averaged before summing with the other strata. The CV of N_a was calculated by using the standard deviation of egg density at age and stratum, weighted by stratum area. The average of the standard deviations was used in the case of the central time strata.

The maximum age of eggs that could be used in estimating daily egg production was the maximum age for which there appeared to be no significant advection out of the survey area owing to water movements (a loss of eggs by advection would cause a negative bias in N_a). Advection was examined by plotting centroids of each age group (Appendix 2) and by using the buoy and CTD data described above.

The daily egg production, N_0 (eggs/day), and instantaneous mortality for eggs, Z (per day), were estimated by maximum likelihood with the mortality model

$$N_a = N_0 e^{-zt},$$

where t = the mean age (days) of age group a (Appendix 3).

The precision of these estimates was estimated by a bootstrap procedure (Appendix 3).

Daily fecundity per female weight

Survey design Female fecundity and ovarian stage samples were taken from trawls from the RV *Tangaroa* on Ritchie Bank from 7 June–6 July and from commercial vessels on 22 June, 11 July, and 13 July (Table 2). Trawling was done during the week before spawning started (8–11 June), to sample total annual fecundity for the AEPM, and from the start of spawning until spent fish were common (20 June–13 July), to sample fecundity reduction for the DFRM. Twenty five of the trawls were from Ritchie Hill (within the area of the central stratum in Fig. 2B) and three were from North Hill, a spur off the north end of Ritchie Bank, about 12 km north of Ritchie Hill (Fig. 2B) where fish were spawning.

Oocyte sampling, ovarian staging, and daily fecundity estimation The oocytes of 569 mature fish (about 35 fish/trawl) in macroscopic ovarian stages 3 (late vitellogenic, prespawning), 4 (hydrated), 5 (ovulated), or 8 (late vitellogenic, partially spent) were counted. Of these, 218 fish were prespawning and used for total annual fecundity analysis. The remainder were used for DFRM analysis. Oocytes were counted by using the automated system described in Appendix 4.

The proportions of females in ovarian stages 3, 4, 5, and 8, and stage 6 (spent) in the trawl samples were estimated by using macroscopic ovarian staging of about 100 randomly chosen females per trawl.

The ovarian stages were further grouped because it was observed that stages 3 and 4 (group 1) had higher fecundities/ kg than stages 5 and 8 (group 2); this difference was due to fish in group 2 having started spawning. Therefore, the estimate of fecundity per female weight, R_i, was stratified by these groupings to minimize error. Stage-6 fish (spent) were placed in group 3. Thus, R_i was estimated as the mean number of eggs/kg of all females that would spawn, were spawning, or were spent, for trawl i:

$$R_i = \frac{\sum_{j=1}^{2} n_{ij} r_{ij}}{\sum_{j=1}^{3} n_{ij}}.$$

Table 2

Trawl stations used for estimation of total annual fecundity for the AEPM and fecundity reduction for the DFRM June–July 1993 on Ritchie Hill (R. Hill) and North Hill (N. Hill) (Fig. 2B). Catches taken on 22 June and 11 and 13 July were from commercial tows and catch sizes were unknown. No. staged = number of fish staged; Immat. = immature; Prop. active = proportion of active fish.

Date	Site	Catch (kg)	No. staged	Immat.	Stage 3	Stage 4	Stage 5	Stage 8	Stage 6	Prop. active
AEPM										
8 Jun	R.Hill	67	26	0	24	2	0	0	0	1.00
8 Jun	R.Hill	30	9	0	8	1	0	0	0	1.00
9 Jun	R.Hill	980	95	0	78	15	0	0	2	0.98
9 Jun	R.Hill	980	95	0	78	15	0	0	2	0.98
11 Jun	R.Hill	35	10	0	9	1	0	0	0	1.00
11 Jun	R.Hill	239	88	2	70	11	3	2	0	1.00
11 Jun	N.Hill	7,494	165	2	125	33	4	1	0	1.00
11 Jun	R.Hill	549	81	1	67	13	0	0	0	1.00
14 Jun	R.Hill	122	41	1	28	7	4	1	0	1.00
14 Jun	R.Hill	103	31	3	22	5	0	1	0	1.00
14 Jun	R.Hill	573	75	0	51	17	3	4	0	1.00
15 Jun	R.Hill	1,195	77	0	51	21	1	4	0	1.00
15 Jun	R.Hill	82	23	0	10	8	2	3	0	1.00
16 Jun	R.Hill	47	14	1	9	2	0	2	0	1.00
16 Jun	N.Hill	3,634	63	1	25	23	10	3	1	0.98
17 Jun	R.Hill	21,478	214	0	90	96	24	4	0	1.00
17 Jun	R.Hill	215	63	2	30	21	9	1	0	1.00
DFRM										
20 Jun	R.Hill	23,535	139	0	31	85	22	1	0	1.00
22 Jun	R.Hill	unknown	107	0	19	83	4	1	0	1.00
27 Jun	R.Hill	7,218	83	0	6	26	39	10	2	0.98
27 Jun	R.Hill	33,975	227	0	10	128	78	8	3	0.99
30 Jun	R.Hill	19,405	135	0	3	50	69	8	5	0.96
2 Jul	R.Hill	7,797	45	0	3	12	22	5	3	0.93
4 Jul	R.Hill	2,936	147	0	1	67	50	13	16	0.89
6 Jul	N.Hill	25,400	56	0	0	7	27	10	12	0.79
6 Jul	R.Hill	402	83	0	0	2	57	19	5	0.94
11 Jul	R.Hill	unknown	31	0	0	2	15	3	11	0.65
13 Jul	R.Hill	unknown	77	0	0	6	31	11	29	0.62

where n_{ij} = number of fish of ovarian group j at station i; and

r_{ij} = mean fecundity (eggs/kg) of fish of ovarian group j at station i.

The mean fecundities/kg of fish of ovarian groups 1 and 2 (r_{ij}) were estimated as

$$r_{ij} = \frac{\sum_{k=1}^{m_{ij}} e_{ijk}}{\sum_{k=1}^{m_{ij}} w_{ijk}},$$

where e_{ijk} = total fecundity of the kth fish of group j in the fecundity sample from station i (adjusted by the gonad wall proportions of total ovary weight in Appendix 4);

w_{ijk} = body weight (kg) of the kth fish of group j in the fecundity sample from station i; and

m_{ij} = number of fish of group j in the fecundity sample from station i.

The R_i's from the 11 DFRM trawls were fitted with a linear regression against time (weighted by the total number of fish in the ovarian-stage sample for each R_i) to estimate D, which is the mean daily fecundity (eggs/(kg × day)) for mature fish. The CV of D was estimated as the standard error of the slope of the regression, divided by the slope.

Biomass of spawning females

The biomass of spawning females B_{spf} was calculated by using the DFRM model given above. The CV of

B_{spf} was determined from the standard error of 1,000 estimates of B_{spf}, formed by dividing the 1,000 estimates of N_0 (Appendix 2) by 1,000 normally distributed estimates of D, formed from the mean and standard error of D.

Proportions spawning, recruited, and female

The scaling factors needed for converting the biomass estimate of Ritchie Bank spawning females to one for recruited fish (≥32 cm SL for both sexes) for the entire mid-east coast stock were estimated from the March–April 1993 wide-area east coast trawl survey (Field et al.[2]), instead of from the trawl data gathered at the time of the egg survey, for two reasons. First, not all recruited fish spawn each year (and thus may not migrate to Ritchie Hill). Second, a more precise estimate of sex ratio is available from the trawl survey than from the relatively few trawls carried out during spawning (when sex ratios are most variable; Zeldis, 1993). The trawls from the wide-area survey used for the scaling factors were those from over the entire mid-east coast survey area, from just north of Ritchie Bank, south to Banks Peninsula (Fig. 1; quota management areas 2A South, 2B, and 3A, respectively). This is the likely distribution of the stock that migrates to the Ritchie Bank to spawn.[10] No spawning orange roughy have been located in areas 2B or 3A, and genetic data show that orange roughy from these three areas cannot be separated, whereas they are genetically distinct from orange roughy on Chatham Rise (Fig. 1).

Stage-3 (late vitellogenic) females in each trawl in the 1993 wide-area trawl survey were assumed to be those that would spawn that year (Bell et al., 1992). Because ovaries of stage-3 females are indistinguishable macroscopically from ovaries of fish in which massive atresia has occurred (Bell et al., 1992), the macroscopic staging was checked by histological examination of about 20 stage-3 fish collected on each day of the 28-day trawl survey.

Recruited biomass

The scalar (S) was calculated as

$$\frac{\sum_i \left(P_{rec,i} C_i \frac{A_i}{n_i}\right)}{\sum_i \left(P_{spf,i} C_i \frac{A_i}{n_i}\right)},$$

where $P_{rec,i}$ and $P_{spf,i}$ = the proportions (by weight) of recruited fish and spawning (stage-3) females, respectively, in the catch from the ith trawl;

C_i = the catch rate (t/nmi) at the ith trawl;

A_i = the stratum area for the stratum containing the ith trawl; and

n_i = the number of trawls for the stratum containing the ith trawl.

The precision of the estimates of S was estimated by using the following bootstrap procedure. For each trawl, the triplet (X_i, $P_{rec,i}$, $P_{spf,i}$) was calculated, where $X_i = C_i A_i / n_i$. One thousand simulated data sets were generated by drawing triplets at random with replacement. Each simulated survey contained the same number of trawls as the area of the original trawl survey. For each simulated survey a bootstrap estimate of S was calculated as

$$\frac{\sum_i (P_{rec,i} X_i)}{\sum_i (P_{spf,i} X_i)},$$

The bootstrap estimates of S were used to calculate a CV for S.

The recruited biomass, B_{rec}, was calculated by using the DFRM biomass model given above. The bootstrap estimates for S were combined with the bootstrap estimates of B_{spf} to obtain a CV for B_{rec}.

Results

Daily planktonic egg production

Planktonic eggs were first captured in very low numbers on 15 June during subsurvey 1 (Fig. 3). Egg abundance remained low until the end of subsurvey 2 (25 June). This subsurvey was prolonged by ship and sampling-equipment breakdowns, and only the central strata, two of the middle strata, and none of the outer strata were sampled. The breakdowns prevented further sampling until the start of subsurvey 3 on 28 June, when large quantities of eggs were captured. Catches then decreased during subsurvey 4 (ending 6 July). Sampling of subsurveys 3 and 4 was completed. In subsurvey 5, only the central stratum and one middle stratum were occupied before the scheduled survey period ended on 7 July. Egg production continued at this time.

[10] Annala, J. H., and K. J. Sullivan (compilers). 1996. Report from the Fishery Assessment Plenary, April–May 1996: stock assessments and yield estimates, 308 p. Unpubl. report held in NIWA Library, Wellington, New Zealand.

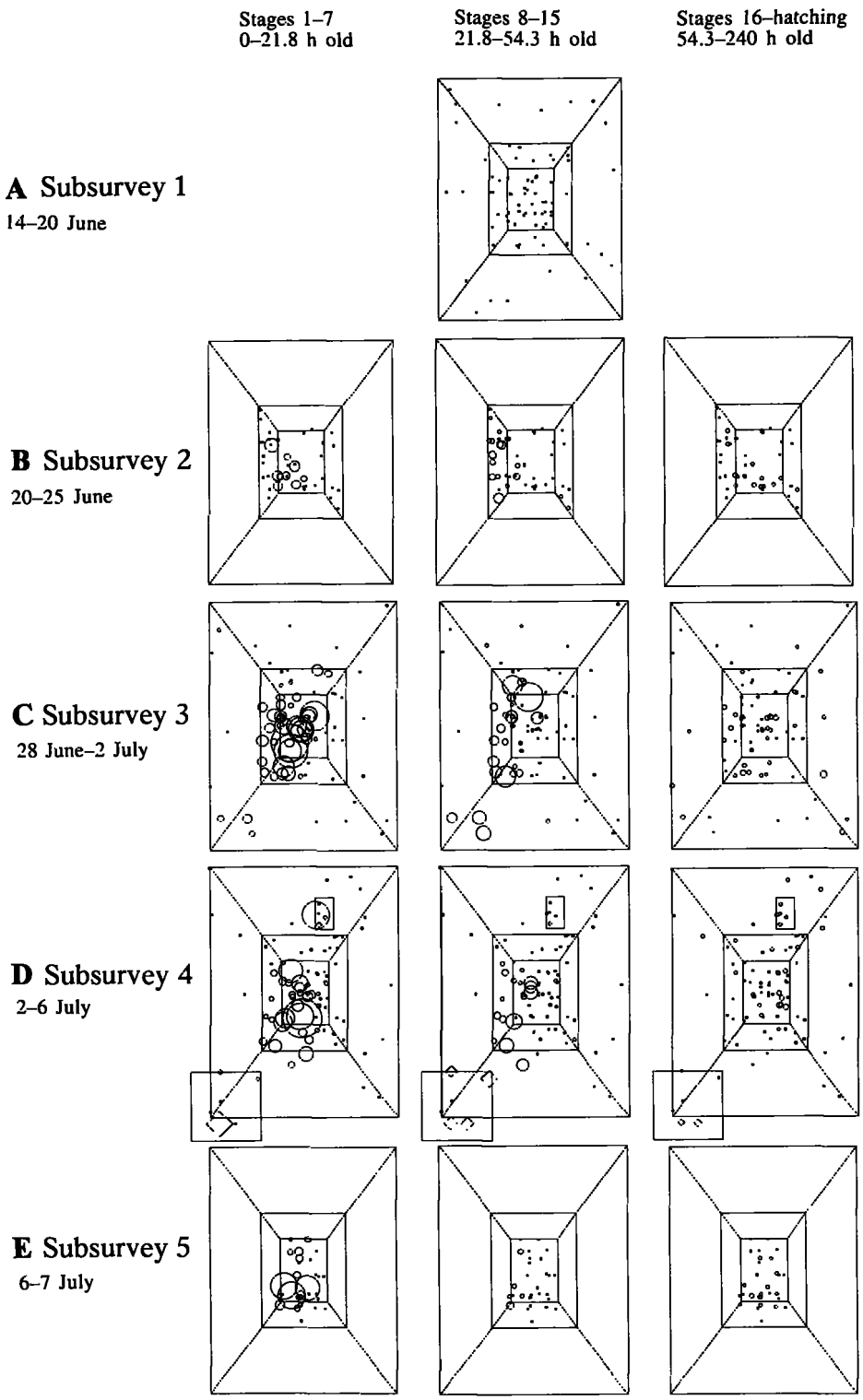

Figure 3

Positions and egg catch rates (m^2) for plankton tows by subsurvey and egg age group. In all panels (**A–E**), catch rates are proportional to circle area (zero catches are filled dots). Only six eggs were caught in subsurvey 1 (A); therefore only one panel was used to show station positions. The extra stations (diamonds) and strata were added after completion of subsurvey 4 shown in (D). The largest symbol in the figure = 310 eggs/m^2 sea surface area. Refer to Figure 2 for the plankton survey location and bathymetry.

Data from the completed subsurveys 3 and 4 showed that egg catches were highest in the central and middle strata (Fig. 3, C and D). These eggs were predominately in the young, grouped-age category (stage 7 or less, ≤21.8 h old; Table 1), but many middle-aged and some older eggs were also caught in these strata. A few orange roughy yolk-sac larvae were also caught in the central and middle strata. These high catch rates for eggs were spatially correlated with high research trawl catch rates for adults (Fig. 2, A and B; Table 2). Catches in the outer strata were usually <10 eggs/tow or zero eggs/tow. However, there was one large catch of young eggs near North Hill (Fig. 3D), on which relatively large catches of spawning adults were made with research trawling (Table 2) and commercial trawling. All of the undamaged eggs in this sample (19% of all eggs) were at the 1-cell stage, indicating that these eggs arose from localized spawning on North Hill. Four additional random tows were then made within an extra stratum created in this area (Fig. 3D) at the end of subsurvey 4. Only 5 additional eggs in total were caught in these tows, indicating that egg production on North Hill was low compared with that on Ritchie Hill.

A few moderate egg catches were also made in the southwestern corner of the survey area (Fig. 3, C and D). Most of these eggs (84%) were > stage 7. Four additional tows were then made within an extra stratum created in this area (Fig. 3D) at the end of subsurvey 4, and in three of these tows, all eggs were > stage 7. The fourth sample had many damaged eggs (≤ stage 7), but it was likely that these were at the older end of the age range of "young" eggs, judging by the stages of undamaged young eggs in that sample (all were ≥ stage 5). The bottom in the area where these samples were taken (Fig. 2B) is deeper (>1,000 m) than depths at which orange roughy normally spawn (850–900 m), and trawl catch rates in the area were very low in this survey and in previous surveys (Fig. 2, A and B). This finding indicated that these eggs had not been produced locally, but rather had been advected from the main spawning center on Ritchie Hill.

The positions of the centroids (centers of gravity) of successive egg age groups suggested that advection was initially to the southwest out of the survey area (Fig. 4A) but that older eggs (those of the very-broad-age-group stage 16+, ≥54.3 h old; Table 1) reentered the area, possibly from the east. In interpreting Figure 4, it is important to realize that centroids close to the boundary of the survey area were unlikely because only eggs from within the survey area were used in the calculation of centroid position. An estimate of the average rate of advection, at the depths of these egg stages, was calculated by dividing the distance between the centroids of stages ≤7 and 11 by the difference between the mean ages in these two age groups (Appendix 3) and was found to be 7.4 cm/sec.

The distribution of eggs by age within the survey area (Fig. 4, B and C) confirmed the southwesterly drift pattern. Eggs ≥ stage 11 (≥ 28.4 h old) became increasingly centered in the southwestern corner of the survey area (region 1, Fig. 4, B and C). However, the old eggs in the stage 16+ group were most abundant in the eastern and central regions (Fig. 4, B and C).

The advection inferred from egg distributions can be compared with hydrographic results. The drogued buoy was relocated 11.2 km south-southwest (bearing=207°) of the release site after 20 h at liberty (Fig. 5A), indicating that advection (at 100 m depth) was to the south-southwest, at a rate of 16 cm/sec. Geostrophic analysis of the CTD data (Fig. 5, A–D) indicated that in the northern part of the station grid (in the vicinity of the Ritchie Hill spawning site), current directions turned from south-southeast through south to southwest as depth increased from 100 through 400 to 800 m. The southwestern component of current velocity between 800 and 400 m (the approximate depth range of eggs ≤ stage 11; Table 1) in the vicinity of Ritchie Hill averaged about 7 cm/sec (Fig. 5D). Geostrophic current speeds averaged about 12–13 cm/sec in the upper 100 m of the water column, in the vicinity of Ritchie Hill. These speeds were probably underestimates because the velocity profiles showed little evidence of reaching asymptotically low values as the postulated level of no motion (1,000 m) was approached (Fig. 5D), suggesting that some residual velocity existed at that level. This may explain the greater buoy speed than geostrophic speed at 100 m. Current speeds toward the southwest (Fig. 5D) were higher on the northern side of the grid than on the southern side through the upper water column; a significant easterly component was observed in the upper 200 m.

Thus, the advection pattern indicated by egg centroids and stage distributions (Fig. 4, A and C) was consistent with results from the drogued buoy (Fig. 5A) and the geostrophic analysis (Fig. 5, A–D), which indicated that the direction of drift of young eggs in the lower half of the water column was toward the southwest. The geostrophic velocities in the lower half of the water column in the vicinity of Ritchie Hill (at least 7 cm/sec) were consistent with the velocity of egg advection (7.4 cm/sec) from our calculations. The older eggs, which would have spent most of their time in the mixed layer (Zeldis et al., 1995), might have been conveyed into the survey area from

the east by a return flow in the upper water column to the south and east of Ritchie Hill.

Egg abundances over the survey area during subsurveys 3 and 4 were calculated by using the curved and straight trajectory assumptions (Table 3). The ratios of the curved and straight abundances generally decreased with egg stage. This decrease was expected because the curved trajectory is nearer to vertical deeper in the water column (where the younger eggs are) than shallower in the column (where the older eggs are). The curved and straight trajectories tended to be nearly parallel in shallower water.

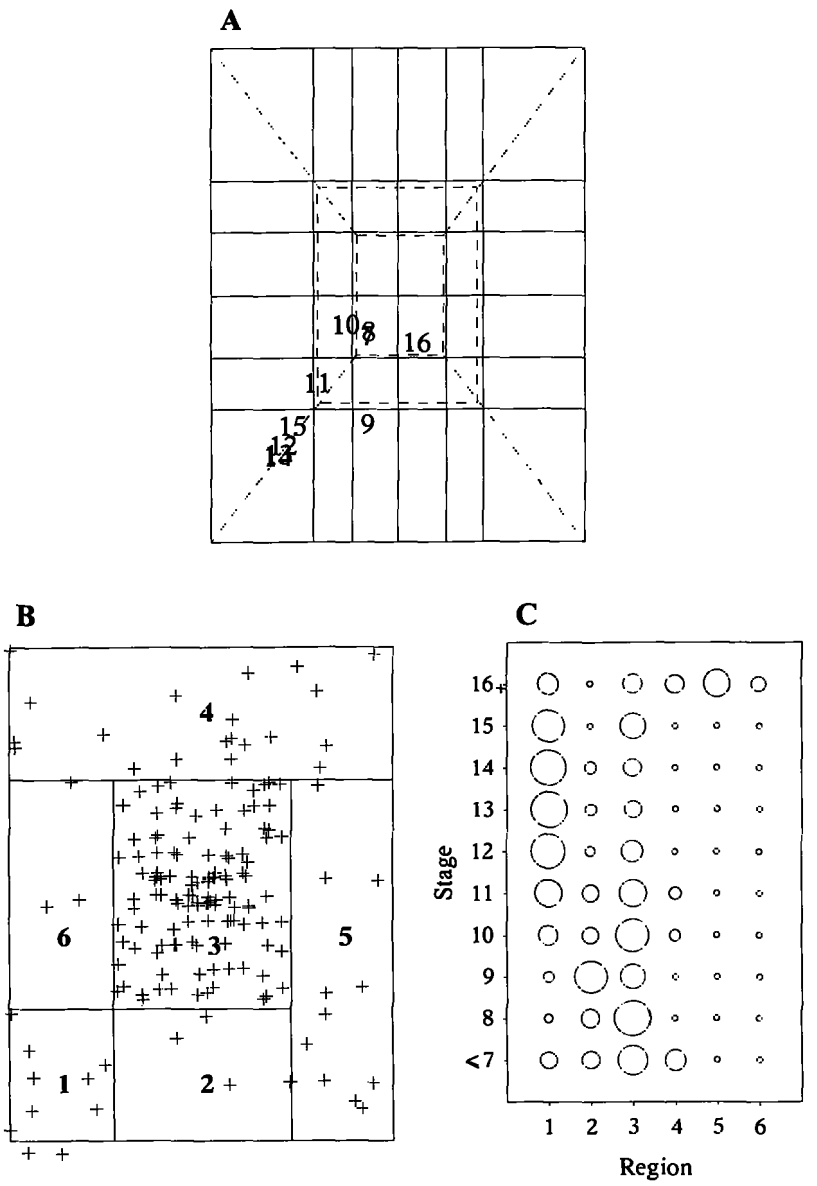

Figure 4

Studies of egg-stage distributions derived from subsurveys 3 and 4. (**A**) The positions of centroids of the egg stages and the 36 subareas of the plankton survey area (solid lines) used in calculating centroid positions (Appendix 2). Centroid 7 represents the combined stage group 1–7, and centroid 16 represents stages 16 to 29 (hatching). The stratum boundaries of the survey area (dotted lines, slightly offset) are shown for reference. (**B**) Six regions and stations used in the distribution analysis (region 3 comprised the inner and middle strata of the survey area), including the extra stations allocated in the southwestern corner. These latter stations were assumed to lie within region 1 for this analysis. (**C**) Proportions (circle areas) of eggs within the regions in B, by egg stage.

Because eggs were advecting into the southwestern corner of the survey area (region 1, Fig. 4C) by the time they reached stage 11, only stages ≤10 were used in the estimation of daily egg production. The criterion used for this cutoff stage was that all stages ≥ the first stage to have >20% of their abundance in region 1 would be excluded from the analysis. This criterion was reached at stage 11. Using the abundance data calculated by assuming a curved net trajectory (Table 3), we estimated that egg production was $N_0 = 10.9 \times 10^9$ eggs/day (CV=0.46) and that the mortality-rate estimate was Z = 0.70/day (CV=0.69) (Fig. 6; Table 4). These calculations used the extra strata at North Hill and in the southwest, and all stations in subsurveys 3 and 4 falling within these strata were considered to have been originally selected within them. The N_0 estimated by assuming a straight trajectory was 8.0×10^9 eggs/day (CV=0.49) with $Z = 0.56$ (CV=0.88). In the remaining analyses, the N_0 value calculated by assuming a curved trajectory was used because this value was likely to be a better approximation to the truth than that obtained by assuming a straight trajectory.

Daily fecundity of females

The proportions of females in each ovarian stage in each DFRM trawl (Fig. 7) showed that the female population was, at first, nearly all in the prespawning state (stage 3). Maxima of hydrated, ovulated, and

spent proportions followed at approximately 10–15 day intervals. Serial spawning was evident in that partially spent, hydrated, and ovulated proportions became fairly constant during a 10-day period (roughly 25 June–5 July) when ovaries of the fish were developing among these stages. Hydration did not appear to be associated with imminent spawning, because significant proportions (0.15) of hydrated fish were present about 5 days before planktonic eggs were first caught on 15 June. However, the first appearance of significant proportions (>0.05) of ovulated fish (14 June) and planktonic eggs (15 June) nearly coincided.

The decline in R_i (Fig. 8) or the daily fecundity per female weight, D, was 787 eggs/(kg × day) (CV= 0.11; Table 4).

Ritchie Bank spawning female biomass

When N_0 was divided by D, the estimate of B_{spf} was 14,000 tons (Table 4), with CV = 0.50.

Biomass of recruited orange roughy in the mid-east coast stock

The factor S was estimated to be 1.77, with CV = 0.03. However, histology showed that for 4.5% of the females identified as spawners in the wide area trawl survey, their entire exogenous vitellogenic oocyte complement was actually in the process of atresia (Bell et al., 1992). These fish were indistinguishable macroscopically from fish that would spawn successfully and did not appear to cluster in any particular area of the trawl survey. The factor S was scaled upward to account for these fish, resulting in S = 1.85 (Table 4).

The resulting estimate of B_{rec} was 26,000 t (Table 4), with CV = 0.50. The bootstrap procedure used may have slightly overestimated the CV of S because it did not fully take into account the stratum structure of the wide-area survey. However, this overestimation is of little importance because the CV of S was so much smaller than that of the other components that made up the CV of B_{rec} (Table 4).

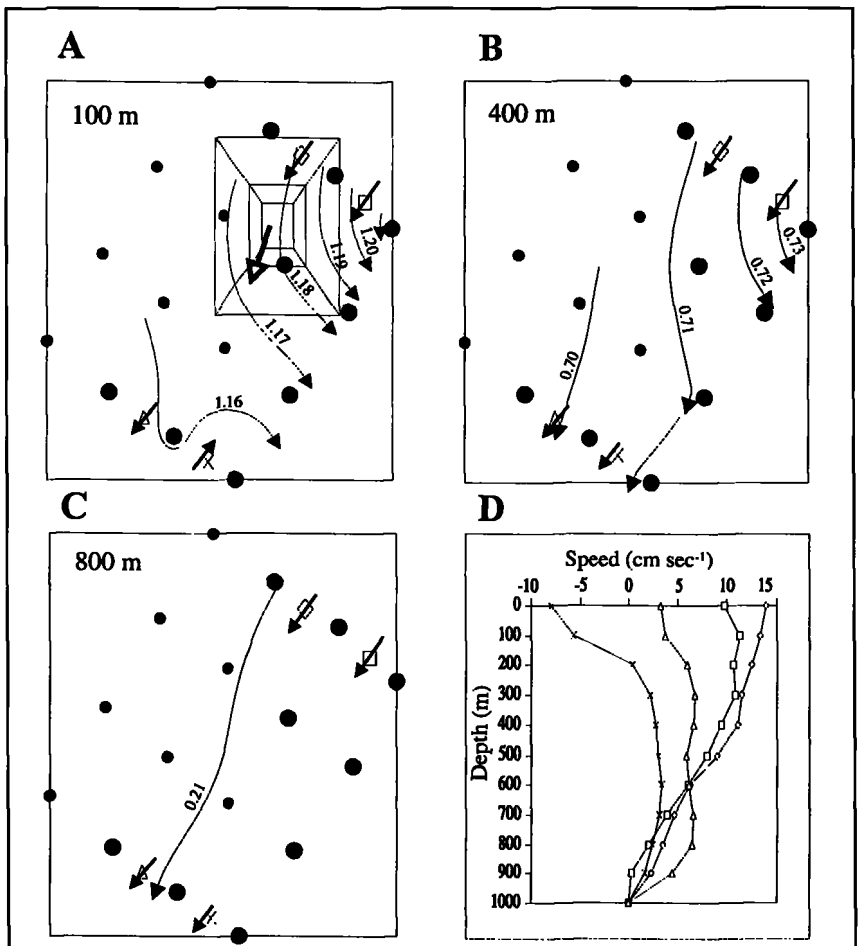

Figure 5

Contours of dynamic height (dynamic meters) at 100, 400, and 800 m in the hydrographic survey area (**A–C**). The arrows on the contours show inferred current directions. The large filled circles indicate stations used in the analysis (where cast depths were ≥ the 1,000 m reference depth). Panel (**D**) shows depth profiles of current velocity (cm/sec) at the symbols in A–C, flowing in the direction of the arrows through each symbol. In A, the plankton survey area is shown for reference and the start and end positions of the buoy deployment are shown by the beginning and end of the open-headed arrow.

Bias due to turnover

An important potential bias in the DFRM arises from the fact that the method is sensitive to turnover of fish on the spawning ground. For example, if fish arrive, complete spawning, and leave the trawl survey area *before* or *after* the trawl survey period, fecundity will be undetected and biomass will be underestimated. These effects were unlikely, however. Almost no eggs were caught in the first subsurvey (Fig. 3A), and very few spent fish were detected in trawls on Ritchie Hill until 2 July (Fig. 7). This finding suggested that no spawning was completed before the trawl survey began (8 June). In addition,

Table 3

Abundances of eggs ($\times 10^{-6}$) and coefficients of variation (CV) at stage, during DFRM planktonic egg survey, calculated with curved and straight net trajectory assumptions. Also given are the ratios of curved and straight abundances.

Stage	Curved abund.	CV	Straight abund.	CV	Ratios
≤7	7,036	0.26	5,453	0.28	1.29
8	487	0.40	424	0.43	1.15
9	673	0.60	451	0.51	1.49
10	316	0.43	276	0.49	1.15
11	400	0.24	351	0.26	1.14
12	1,420	0.32	1,276	0.32	1.11
13	740	0.23	716	0.24	1.03
14	276	0.38	260	0.37	1.06
15	34	0.42	38	0.38	0.90

proportions of macroscopic stage-3 (vitellogenic) fish declined to 5% by the midpoint of the trawl survey period and to 0% by the end; stage-4 (hydrated) fish showed a similar decreasing trend. Thus no prespawning fish were present at the end of the trawl survey (13 July).

Turnover during the trawl survey period may have biased the biomass estimate if prespawning fish arrived late to the trawl survey area (after trawling for R_i had started), at the beginning of the season. This means that not all prespawning fish would have been sampled by trawls in the spawning area, which would cause an underestimate of R_i, because fish that had started spawning would be over-represented. Similarly, if spent fish departed the trawl survey area early (before trawling for R_i had ended) toward the end of the season, spent fish would be under-represented by trawls in the spawning area. In this case, R_i would be overestimated because fish which had not finished spawning would be over-represented. Both of these effects (late arrivals and early departures) would cause an underestimate of D, which, in turn, would cause an overestimate of biomass, N_0/D.

Was it likely that late arrivals or early departures (or both) of spawners occurred in the present study? The annual fecundity/kg of prespawners, estimated from fish sampled before the R_i sampling period and before any eggs were caught in the plankton (Fig. 8), was 27,271 eggs/(kg × yr). If this estimate is divided by the estimated daily fecundity/kg (787 eggs/(kg × day); Table 4), the period required for the average fish to spawn completely is 35 days. However, the time lag between the first appearance of significant proportions (>0.05) of ovulated and spent fish was about 19 days (from 14 June to 2 July; Fig. 7). If this lag is interpreted as the duration of spawning in individual fish, D was underestimated by the fecundity reduction trawling.

It would appear, however, that late arrival of prespawners to the trawling area did not contribute greatly to the underestimation of D. The R_i sampling period began on 20 June when prespawner (stage-3) proportions had become low (0.20; Fig. 7) and were decreasing rapidly. At this time the estimated R_i was only about 10% below the prespawning level (Fig. 8). Eggs first appeared in the plankton on 15 June, but catches of young eggs in the central strata were still relatively small (3.9 eggs/m^2; Table 5) during 20–25 June (subsurvey 2). Therefore, only a relatively small reduction in R_i would have been expected by

Table 4

Parameter estimates for DFRM for Ritchie Hill spawning female biomass and mid-east coast recruited biomass, June–July 1993 (with coefficients of variation in parentheses). N_0 = daily egg production for Ritchie Hill survey area (estimated with curved net trajectory); D = weight specific daily fecundity of females; B_{spf} = biomass of spawning females in Ritchie Hill survey area; S = ratio of recruited biomass to that of spawning females; B_{rec} = biomass of recruited fish. Parameter estimates with subscripts marked "*turn*" have turnover incorporated (see text); CV's were not estimated in these cases.

Parameter	Estimate
N_0	10.9×10^9 eggs/day (0.46)
D	787 eggs/(kg × day) (0.11)
B_{spf}	14,000 t (0.50)
S	1.85 (0.03)
B_{rec}	26,000 (0.50)
D_{turn}	1,106 eggs/(kg × day)
$B_{spf,\,turn}$	9,900 t
$B_{rec,turn}$	18,200 t

Table 5

Mean abundances (per m^2) of all eggs ≤ stage 7 and dates of sampling in the central strata for each subsurvey.

Subsurvey	Date	Mean	CV
1	15–17 June	0.0	0.0
2	20–25 June	3.9	0.34
3	29 June–1 July	49.0	0.29
4	3–5 July	22.6	0.46
5	6–7 July	22.2	0.50
4 and 5	3–7 July	22.4	0.34

20 June, in agreement with the reduction actually observed by that date (Fig. 8).

It was likely, however, that early departures caused spent fish to be under-represented in the trawl samples toward the end of the R_i time series. The abundance of young planktonic eggs in the central strata was reduced by more than half between subsurvey 3 (mid-date 30 June) and subsurvey 4 (mid-date 4 July; Table 5). Because subsurvey 3 was done when the spent proportion was virtually zero (Fig. 7), this reduction of planktonic egg abundance implied that about half of the fish had ceased spawning by 4 July (assuming that the spawning rate of remaining active fish was constant). However, only 0.11 of fish were recorded as spent on 4 July (Table 2; Fig. 7); thus this proportion appeared to be underestimated by 0.50 – 0.11 = 0.39 on 4 July. Commercial catch rates on Ritchie Hill (Fig. 9) also decreased considerably during the last week of June and first week of July, suggesting that fish abundance in the trawling area had declined.

To account for the error in D that the underestimation of spent fish would cause, the proportion of active fish on 4 July was adjusted downward to 0.89 – 0.39 = 0.50 to estimate a new D value of 1,106 eggs/(kg × day) (assuming a linear decline between 20 June and 4 July; Fig. 8; Table 4). This adjustment resulted in a period of 25 days for an average fish to spawn completely, which is not greatly different from the 19 days estimated from the time lag between ovulated and spent fish proportions (shown above). This re-estimation of D, to account for turnover, had proportional effects on B_{spf} and B_{rec} (Table 4).

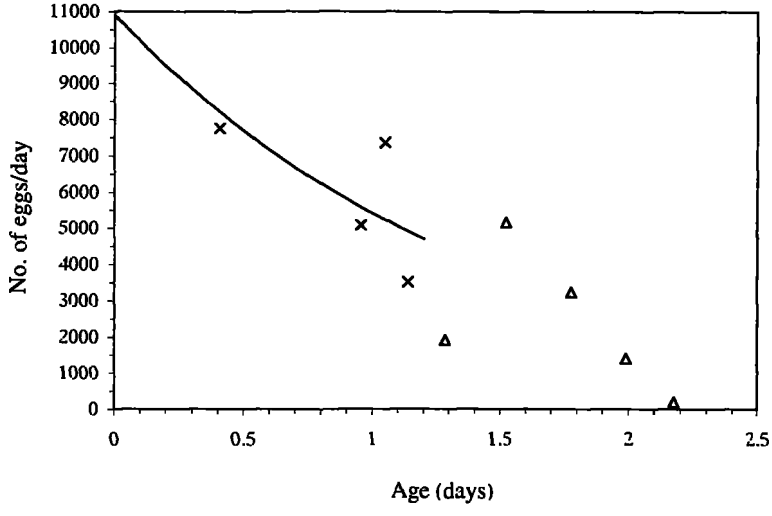

Figure 6

The daily production of eggs as a function of age, calculated by dividing the curved trajectory egg-abundance estimates (Table 3) by the duration of each age group and by plotting against the mean age of eggs in each age group (Appendix 3). The line was fitted by using N_0 and Z (Appendix 3), calculated with only egg stages ≤ 7 to 10 (crosses). Egg stages 11 to 15 (triangles), were not used in the production estimate because they were subject to advection out of the survey area (see text).

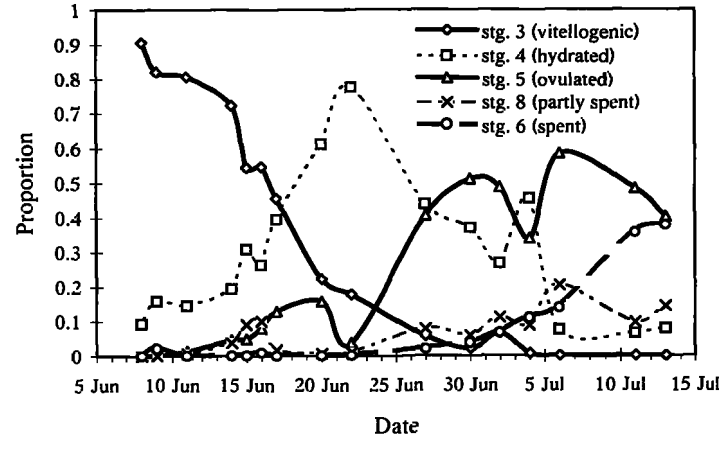

Figure 7

Time series of macroscopic ovarian stages over the survey period. Each point is the proportion of females at that stage, as a proportion of all mature females, averaged for all trawls on that date. Only trawls on Ritchie and North Hills were used (Table 2).

Discussion

This study has used the DFRM to estimate the biomass of recruited individuals in the mid-east coast orange roughy stock, by combining estimates of daily egg production rate, the rate of fecundity reduction, and the proportion of the stock that was spawning females. In this section various sources of error are discussed, and the methods and results of this study are compared with those of other studies. Also, a brief description is made of how the results from this survey have been used in assessing the stock.

Sources of error

In egg-production surveys, the trajectory of the plankton net during deployment and retrieval is usually assumed to be straight (and often, vertical). The analyses presented here (Appendix 1) suggest that, for the present survey, 1) there was significant horizontal movement of the net during deployment owing to drag from the warp (which was caused by ship drift), and 2) the plankton net followed a curved trajectory during hauling. The curved trajectory meant that less water was filtered in deeper than in shallower ocean layers of equal thickness and that larger correction factors were required for younger (deeper) eggs in order to standardize the egg counts to eggs/m^2. The effect of using curved, rather than straight, trajectories was to increase the estimated production rate by 36% (from 8.0 to 10.9 billion eggs/day). Recent egg-production survey work, using a digitally recording flowmeter system developed at NIWA (Grimes[9]), has shown that 1) there often are spurious revolutions of the flowmeter on the downcast, negating the use of conventional flowmeters and that 2) more water is filtered at shallower depths than at deeper depths, justifying the assumption of a curved net trajectory. Therefore, it is likely that by allowing depth variation in the estimates of the amount of water filtered, a major improvement was made over the assumption of a straight net trajectory.

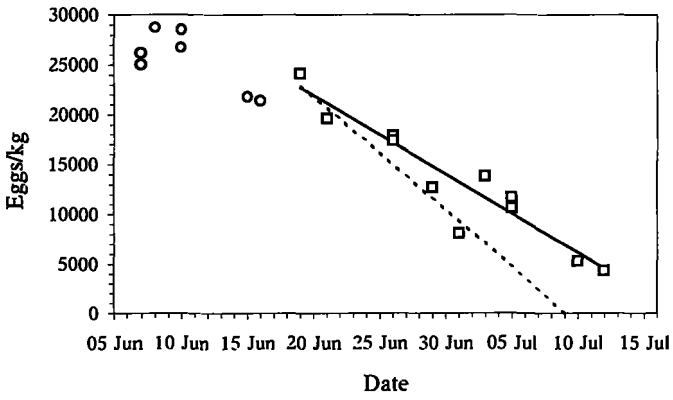

Figure 8

Weight-specific fecundity (eggs/kg spawning female: R_i) from trawls prior and during the DFRM sampling period (circles and squares, respectively, Table 2). Solid line is a weighted linear regression fitted for DFRM trawls. Dotted line is a regression fitted when it was assumed that proportion active was overestimated by 39% on 4 July (see text).

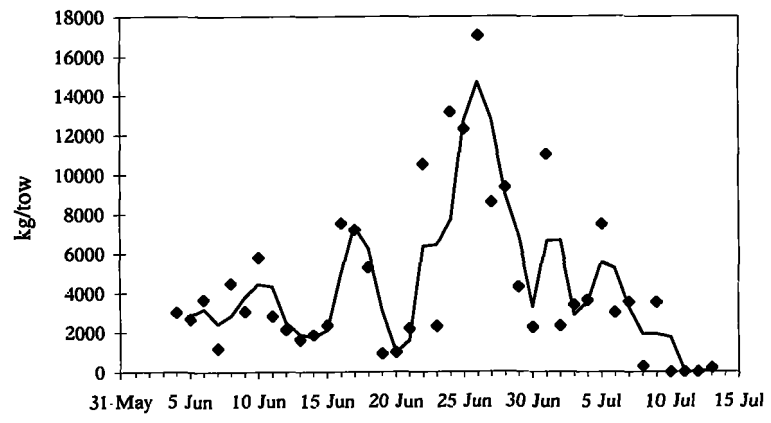

Figure 9

Commercial catch rates of orange roughy, *Hoplostethus atlanticus*, on Ritchie and North Hills, 4 June–13 July 1993. Points are the means of all catches by all vessels on each day (kg/tow), fitted with a moving average (line) with a 2-day period.

The precision of the planktonic egg production estimate was influenced by damage to early stage eggs (Zeldis et al., 1995; Grimes et al.[3]). In the present study, the inability to stage most eggs less than 21.8 h old caused a greater reliance on older egg stages to estimate production. However, the number of older egg stages that could be used for the estimation was limited because eggs older than stage 10 (28.4 h) were subjected to advection toward and through the southwestern boundary of the survey area as they aged. Thus, the original strategy of making the survey area large enough to retain all of the eggs up to 36 h old was defeated, and relatively few stages were available for a mortality estimate. Clearly, the combination of nearly concurrent information on ocean circulation (from CTD and drogued buoy) and on the drift patterns of the eggs themselves provided useful corroborative information for quantitative decisions about the egg-age range available for mortality estimation, when eggs were subject to advection.

Precision estimates for the egg-abundance data may have been biased by potential autocorrelation among the data, which would not bias the esti-

mate of egg production but could cause its precision to be overestimated. No attempt was made to correct for this bias because the data were judged to be inadequate to estimate an autocorrelation structure (which would need to have both spatial and temporal terms). Picquelle and Megrey (1993) drew the same conclusion for pollock egg surveys. For the present study, a minimum spacing of 1,000 m was imposed when allocating the stations to the strata. This spacing should have gone some way toward minimizing the effects of spatial autocorrelation. In an explicit study of autocorrelation in anchovy egg catches, Smith and Hewitt (1985) found that spatial autocorrelation diminished rapidly at spatial scales of 2,000 m and that temporal autocorrelation diminished at 0.5 h for 1-day-old eggs. Given that the minimum distances and times between samples for the egg stages used in this study were of this order and that the egg catch rates were highly variable, overestimation of precision was likely to be minor.

Use of the DFRM required the assumption that the 11 trawls used to estimate D representatively sampled spawning females on Ritchie and North Hills. Although it is clear that spawning female biomass is highly aggregated in the Ritchie Hill area (Fig. 2), it is not known to what extent females are randomly distributed within this small area, with respect to ovarian stage. Therefore, it was useful to look at a much larger set of fecundity data collected on these hills in 1995 by N.Z. Ministry of Fisheries (MOF) scientific observers working on commercial vessels (Zeldis, unpubl. data). Samples were taken from 47 trawls made with four vessels (range of 7–16 trawls per vessel) throughout the entire spawning season. These tows were long, typically traversing much of the ridge between North Hill and the south side of Ritchie Hill (Fig. 2) and covering the 850–900 m depth range of orange roughy spawning. The fecundity reduction rate from these 1995 data (uncorrected for turnover) was 965 eggs/(kg × day) (CV=0.11), which was not significantly different from the uncorrected estimate from 1993 in the present study, 787 eggs/(kg × day) (CV=0.11; Table 4). This rate showed that widespread and intensive trawling in this area would yield an estimate of D similar to that from the less intensive research trawling of the present study, indicating that the less intensive trawling accurately represented the spawning dynamics of the population.

The reliance of the DFRM on within-spawning season trawl data makes it susceptible to bias due to turnover, which causes an underestimate of fecundity reduction rate. In the present study, it appeared that spent females left the survey area during the period when fecundity reduction was measured, such that only 0.11 of remaining females were spent 21 days after the start of spawning. A similar pattern of low proportion spent was seen in the 1995 Ritchie Bank scientific observer data described above, with proportion spent < 0.20 about 23 days after the onset of spawning. In contrast, in recent NIWA orange roughy egg production surveys done at East Cape in 1995[10] and at the "Graveyard" area on northern Chatham Rise in 1996[11] (Fig. 1), spent proportions were between 0.60 and 0.70 about 20 days after the onset of spawning. This suggested that turnover was less prevalent at these latter sites, an effect which may be related to the fact that although commercial fishing was intensive on Ritchie Bank during the 1993 and 1995 spawning seasons, there was no commercial fishing during the 1995 and 1996 spawning seasons at East Cape and the "Graveyard." Significantly, the value of D at East Cape was 1,036 eggs/(kg × day), with no correction for turnover, which was similar to the turnover-corrected value for the present study at Ritchie Bank of 1,106 eggs(kg × day) (an estimate is not yet available for the "Graveyard"). For this reason, the turnover-corrected fecundity reduction rate estimated for Ritchie Bank in 1993 is considered to be more reliable than the uncorrected estimate and also a reasonably reliable estimate of the true rate of decline in Ritchie Bank population seasonal fecundity.

Comparision with other studies

The first use of the DFRM was by Lo et al. (1992; 1993) to estimate the biomass of a deepwater pleuronectid flatfish, Dover sole (*Microstomus pacificus*), which spawns between 600 and 1,500 m depth on the continental slope of western North America. The model used in the present study to describe the daily fecundity reduction was simpler than that of Lo et al. (1993). It assumed that the fecundity per fish weight was a linear function of time only (fish weight was considered as an additional predictor but did not significantly improve the fit). Lo et al. (1993) assumed that both total fecundity of active females and the fraction of active females (their E_t and G_t) were linear functions of time and fish weight. The former model was used for two reasons. First, in calculating fecundity reduction, there seemed no need to treat active and inactive females separately. Second, in the absence of any evidence of lack of fit, the rule of Occam's razor suggested using the simpler model.

[11] Grimes, P. J. 1996. Voyage Report, TAN9608 (Part II). NIWA unpublished voyage report held in NIWA Library, Greta Point, Wellington, New Zealand, 4 p.

A second difference between the DFRM used here and that of Lo et al. (1993) is the way sex ratio and active female proportion were estimated and brought into the biomass model. In the present study, the proportion of all recruited fish that were spawning females was estimated with parameter S, whereas this proportion was estimated within the R and D parameters in the model of Lo et al. (1993). Orange roughy spawning takes place in dense aggregations that form after the spawners have migrated hundreds of km from the nonspawners. Therefore, it is not possible to estimate the proportion of active females to all recruited fish with the trawls done on the spawning ground during the spawning season (which are used to monitor fecundity reduction). This estimation must be done with a separate trawl survey over the whole stock area, preferably before the spawners have aggregated significantly. In contrast, Dover sole spawning appears to be dispersed over a wide latitudinal area of the North American west coast slope (Lo et al., 1993) and takes place over a long spawning season (6 months; Hunter et al., 1992). In Lo et al. (1993), the spawners were assumed to be dispersed in the same geographic region as the nonspawners during spawning, and therefore sex ratio and proportion active components were estimated from the same trawls that were used to estimate fecundity reduction.

There are few other estimates of planktonic egg mortality (Z) in the literature for deepwater spawners that can be compared with the value (Z=0.7) obtained for orange roughy in this study. Lo et al. (1993) fitted a Pareto decay function to Dover sole egg abundances, in which mortality was allowed to decrease with egg age. Initial mortality was 0.63 which halved by the age of 1 day. Another western North American slope species, sablefish (*Anoplopoma fimbria*), has been the subject of egg-production studies (Moser et al., 1994) and for this species, Z varied between 0.25 and 0.48, depending on region (it should be noted that counts of 1-day-old and 2-day-old eggs were excluded because these eggs were undersampled). Thus, the few Z estimates that exist for other deepwater species indicate variable mortality rates, but that mortalities can be quite high. Orange roughy egg abundance was estimated by Koslow et al. (1995) in their application of the AEPM to orange roughy biomass estimation on St. Helen's Seamount, Tasmania. These authors assumed that mortality in the first 28 h after spawning was zero and that the mean abundance of 0 to 28 h old eggs equalled N_0. This assumption was based on their finding no differences in abundance among fertilization or 1-cell eggs (stages 1 and 2 of the present study) and their subsequent two stages which were 2 cell and 4–128 cells (stages 3 and 4–9, respectively, of the present study; see also Grimes et al.[3]). As mentioned, the differentiation of stages 1–7 was not possible for the great majority of the samples in the 1993 Ritchie Bank survey because of egg damage. However, the probability that the mortality rate estimated from the grouped stages 1–7 and stages 8, 9, and 10 was zero was low (P=0.10).

The procedure used to estimate S, for converting spawning female biomass to recruited biomass, is easily adapted to estimate the proportion of females in the stock area that will spawn in the current year. For the mid-east coast stock in 1993, S was estimated as 0.52 of all mature females (by weight), a result similar to that for orange roughy stocks in southern Australia (0.45, by numbers; Bell et al., 1992). Wide-area trawl surveys of the east coast were also done in March–April of 1992 and 1994,[10] and these yielded similar values for these proportions (0.49 and 0.42 by weight). Also, a low proportion of females with fully atretic ovaries was found (0.045) over the mid-east coast survey area in 1993, again in common with the results of Bell et al. (1992).

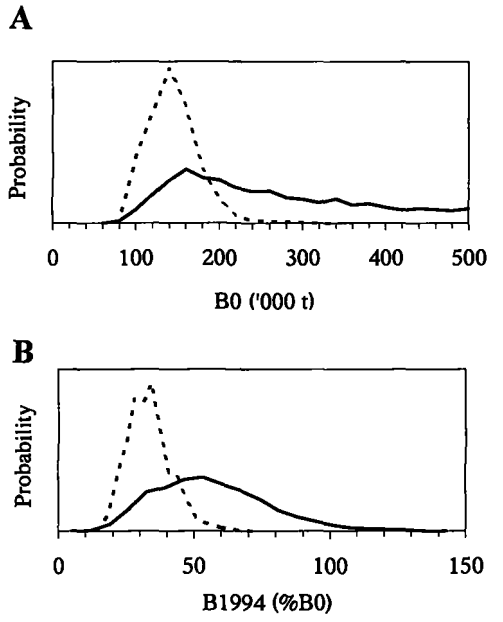

Figure 10

Probability distributions of (**A**) virgin biomass (B_0) and (**B**)1994 biomass as a percentage of B_0, from the 1994 stock reduction analysis for the mid-east coast orange roughy, *Hoplostethus atlanticus*, fishery (see Footnote 2 in the text). Each panel shows (solid line) the distribution when the analysis was done without the DFRM estimate (with only CPUE, trawl survey indices, and mean fish length data) and (dotted line) the distribution when the DFRM estimate was included.

Use in stock assessment

Although the biomass estimates derived from this DFRM survey were rather imprecise (CV=0.50), they were capable of having a dramatic effect on the assessment of the mid-east coast stock. In 1994, an estimate of 45,000 t recruited biomass (CV=0.40) from a preliminary analysis of these data was used in assessing this stock (Field et al.[2]: this estimate differs from those given above because some data errors have subsequently been corrected and the analyses have been refined). The inclusion of this estimate greatly improved the precision of the assessment (Fig. 10), which resulted in a 2-year stepped reduction in TACC from 10,333 t in 1993–94 to 2500 t in 1995–96.

Acknowledgments

The authors would like to thank Kevin Sullivan for statistical advice and revision of the manuscript, Steve Chiswell for assistance with geostrophic analysis, Karen Field for laboratory assistance, and Alan Hart, Jack Fenaughty, and the officers and crew of *Tangaroa* for assistance at sea (all at NIWA). We thank Tony Koslow (CSIRO) for provision of St. Helen's seamount orange roughy egg data, and the external reviewers for their comments. This work was partly funded by the New Zealand Ministry of Fisheries under project DOR609.

Literature cited

Bell, J. D., J. M. Lyle, C. M. Bulman, K. J. Graham, G. M. Newton, and D. C. Smith.
1992. Spatial variation in reproduction, and occurrence on non-reproductive adults, in orange roughy *Hoplostethus atlanticus* Collett (Trachichthyidae), from south-eastern Australia. J. Fish Biol. 40:107–122.

Bycroft, B. L.
1986. A technique for separating and counting rock lobster eggs. N.Z. J. Mar. Freshwater Res. 20:623–626.

Clark, M. R.
1995. Experience with management of orange roughy (*Hoplostethus atlanticus*) in New Zealand waters, and the effects of commercial fishing on stocks over the period 1980–1993. *In* A. G. Hopper (ed.), Deep-water fisheries of the North Atlantic oceanic slope, p. 251–266. Kluwer Academic Publishers.

Francis, R. I. C. C.
1984. An adaptive strategy for stratified random trawl surveys. N.Z. J. Mar. Freshwater Res. 18:59–71.

Hunter, J. R., B. J. Macewicz, N. C. H. Lo, and C. A. Kimbrell.
1992. Fecundity, spawning, and maturity of Dover sole *Microstomus pacificus*, with an evaluation of assumptions and precision. Fish. Bull. 90:101–128.

Hunter, J. R., and N. C.-H. Lo.
1993. Ichthyoplankton methods for estimating fish biomass introduction and terminology. Bull. Mar. Sci. 53(2):723–727.

Koslow, J. A., C. M. Bulman, J. M. Lyle, and K. A. Haskard.
1995. Biomass assessment of a deep-water fish, the orange roughy (*Hoplostethus atlanticus*), based on an egg survey. Mar. Freshwater Res. 46:819–830.

Lo, N. C. H., J. R. Hunter, H. G. Moser, and P. E. Smith.
1992. The daily fecundity reduction method: a new procedure for estimating adult fish biomass. ICES J. Mar. Sci. 49:209–215.

Lo, N. C.-H., J. R. Hunter, H. G. Moser, and P. E. Smith.
1993. A daily fecundity reduction method of biomass estimation with application to Dover sole *Microstomus pacificus*. Bull. Mar. Sci. 53(2):842–863.

Moser, H. G., R. I. Charter, P. E. Smith, N. C. H. Lo, D. A. Ambrose, C. A. Meyer, D. M. Sandknop, and W. Watson.
1994. Early life history of sablefish, *Anoplopoma fimbria*, off Washington, Oregon, and California, with application to biomass estimation. CALCOFI Rep. 35:144–159.

Pankhurst, N. W.
1988. Spawning dynamics of orange roughy, *Hoplostethus atlanticus*, in mid slope waters of New Zealand. Environ. Biol. Fishes 21(2):101–116.

Pankhurst, N. W., P. J. McMillan, and D. M. Tracey.
1987. Seasonal reproductive cycles in three commercially exploited fishes from the slope waters off New Zealand. J. Fish. Biol. 30:193–211.

Picquelle, S. J., and B. A. Megrey.
1993. A preliminary spawning biomass estimate of walleye pollock, *Theragra chalcogramma*, in the Shelikof Strait, Alaska, based on the annual egg production method. Bull. Mar. Sci. 53(2):728–749.

Pond, G. L., and M. A. Pickard.
1978. Introductory dynamic oceanography. Pergamon Press, Oxford, 241 p.

Saville, A.
1964. Estimation of the abundance of a fish stock from egg and larval surveys. Rapp. P.-V. Reun. Cons. Int. Explor. Mer 155:164–173.

Smith, P. E., and R. P. Hewitt.
1985. Anchovy egg dispersal and mortality as inferred from close-interval observations. CalCOFI Rep. 26:97–108.

Tranter, D. J., and P. E. Smith.
1968. Filtration performance. *In* Zooplankton sampling, p. 27–56. UNESCO monographs on oceanographic methodology 2.

Zeldis, J.
1993. The applicability of egg surveys for spawning stock biomass estimation of snapper, orange roughy and hoki in New Zealand. Bull. Mar. Sci. 53(2):864–890.

Zeldis, J., P. J. Grimes, and J. K. V. Ingerson.
1995. Ascent rates, vertical distribution, and a thermal history model of development of orange roughy (*Hoplostethus atlanticus*) eggs in the water column. Fish. Bull. 93(2):373–385.

Appendix 1: Calculation of "curved" correction factors

This appendix describes, for the case where the path of the net during hauling is assumed to be curved, the calculation of the correction factors that convert egg counts to egg density (eggs/m^2).

For each plankton tow, we calculated the following:

1 the position of the net at the start of hauling;
2 the position of the net at a series of equally spaced times during hauling;
3 the flow of water through the net at each of these times; and
4 a correction factor for each of these times.

Finally, interpolation was used to calculate the correction factor when the net was at the mid-point of the depth layer associated with each egg stage. This was taken as the correction factor for that egg stage at that plankton tow.

First, the assumptions behind these calculations and some notation are defined.

Assumptions and notation

The calculations required the following assumptions:

1 the vessel drifted at a constant velocity while shooting and hauling;
2 the net dropped at a constant speed during shooting;
3 the warp was always straight and decreased in length at a constant rate during hauling;
4 the net mouth was always perpendicular to the warp;
5 the water velocity varied only with depth (not with longitude, latitude, or time); and
6 the following are known exactly:
   a) the vessel position at the time of shooting and at the start and finish of hauling,
   b) the net depth and warp length at the start of hauling, and
   c) the water velocity profile.

Two further assumptions are described in sections "Calculating P_{n1}" and "Calculating the net path during hauling."

Let $\underline{P}_n(t)$ and $\underline{P}_v(t)$ be 3-dimensional vectors describing the position of the net and the vessel at time t, where time and position are measured in relation to the time and the vessel position when the net was shot, and where the three coordinates give distances, in meters, to the east, north, and downwards, respectively. (In this Appendix, vectors are underlined to distinguished them from scalars.) Let t_1 and t_2 stand for the times at the start and finish of hauling.

Let the water velocity at depth z be described by the vector $\underline{C}(z)$, and the mean water velocity between the surface and depth z by $\underline{C}'(z)$. Denote the net depth and the warp length at time t by $z_n(t)$ and $w(t)$, respectively (note that $z_n(t)$ is the depth coordinate of $\underline{P}_n(t)$).

Where it is convenient, the symbols t_1 and t_2 will be replaced by subscripts 1 and 2, so that, for example, $\underline{P}_n(t_1)$, $z_n(t_1)$, and $\underline{P}_v(t_2)$ may be written as $\underline{P}_{n1}$, z_{n1}, and $\underline{P}_{v2}$, respectively.

From the above assumptions, $\underline{P}_{v1}$, $\underline{P}_{v2}$, z_{n1}, and w_1 are known, as are $\underline{C}(z)$ and $\underline{C}'(z)$ for all z. Also, of course, $\underline{P}_{n2} = \underline{P}_{v2}$.

Calculating $\underline{P}_{n1}$

In calculating the position of the net at the start of hauling, it was assumed that, while the net was sinking prior to hauling, its horizontal velocity was the sum of the water velocity and some fraction c of the vessel velocity (the latter component being caused by drag from the warp). Thus,

$$\underline{P}_{n1} = c\underline{P}_{v1} + t_1\underline{C}'(Z_{n1}) + \underline{Z}_{n1}, \tag{A1}$$

where $0 \le c \le 1$, and $\underline{Z}_{n1}$ is the 3-dimensional vector, $(0,0,z_{n1})$. Also, from assumptions 3 and 6,

$$\left|\underline{P}_{n1} - \underline{P}_{v1}\right| = w_1. \tag{A2}$$

The value of c (and thus $\underline{P}_{n1}$) can be calculated by solving the simultaneous equations A1 and A2. Geometrically, this is equivalent to finding a point of intersection of the horizontal line defined by Equation A1 and the horizontal circle defined by Equation A2 (both are at depth z_{n1}).

Substituting for $\underline{P}_{n1}$ from Equation A1 in Equation A2 and expanding, we get the quadratic equation in (c–1)

$$\begin{aligned}(c-1)^2\left|\underline{P}_{v1}\right|^2 + 2(c-1)t_1\underline{P}_{v1} \bullet \\ \underline{C}'(z_{n1}) + t_1^2\left|\underline{C}'(z_{n1})\right| + z_{n1}^2 - w_1^2 = 0,\end{aligned} \tag{A3}$$

which is solved with the usual formula ($\bullet$ denotes the vector dot product).

Where there were two solutions for c (at all but a few stations), the one using the negative square root was chosen because it was usually the one that satisifed the condition $0 \le c \le 1$.

For the few stations where Equation A3 had no real solution (i.e. the line and circle did not intersect), $\underline{P}_{n1}$ was taken to be the point on the circle closest to the line. It may be shown that this $\underline{P}_{n1}$ is given by

$$\underline{P}_{n1} = r\frac{\underline{P}_{cl}}{\left|\underline{P}_{cl}\right|} + \underline{P}_{v1} + \underline{Z}_{n1} \tag{A4}$$

where r is the radius of the circle and $\underline{P}_{cl}$ is the point, on the surface vertically above the line, that is closest to the shot position, and is given by

$$\underline{P}_{cl} = t_1\underline{C}'(z_{n1}) - \frac{t_1\underline{C}'(z_{n1}) \bullet \underline{P}_{v1}}{\left|\underline{P}_{v1}\right|^2}\underline{P}_{v1}. \tag{A5}$$

Stations where Equation A3 did not have a real solution, or where c did not satisfy $0 \le c \le 1$, were assumed to be instances where the above assumptions did not hold.

Another situation in which the assumptions clearly did not hold was at the 13 stations where $z_{n1} > w_1$. For these stations, z_{n1} was set equal to w_1, and $\underline{P}_{n1}$ was taken to be vertically below $\underline{P}_{v1}$.

Calculating the net path during hauling

From assumptions 1 and 3, the position of the vessel and length of the warp at any time during hauling was calculated by using

$$\underline{P}_v(t) = \frac{(t_2 - t)\underline{P}_{v1} + (t - t_1)\underline{P}_{v2}}{(t_2 - t_1)} \quad \text{(A6)}$$

and

$$w(t) = \underline{P}_v(t) - \underline{P}_n(t) = \frac{(t_2 - t)w_1}{(t_2 - t_1)}. \quad \text{(A7)}$$

To calculate the position of the net during hauling, we made one further assumption: that the velocity of the net is the sum of the water velocity and a vector in the direction of the warp. With this assumption, an iterative procedure was used to calculate $\underline{P}_n(t)$ at times t_1+*t, t_1+2*t, etc, for a small time interval *t. The basis of this procedure is the ability to calculate $\underline{P}_n(t+*t)$ once $\underline{P}_n(t)$ is known. This is done as follows.

The velocity assumption may written approximately as

$$\frac{\underline{P}_n(t+\delta t) - \underline{P}_n(t)}{\delta t} = p(t)\frac{\underline{P}_v(t) - \underline{P}_n(t)}{\left|\underline{P}_v(t) - \underline{P}_n(t)\right|} + \underline{C}\left(z_n(t)\right), \quad \text{(A8)}$$

where $p(t)$ is an unknown scalar which varies with t. Replacing t by t+*t in Equation A7, we get

$$\left|\underline{P}_v(t+\delta t) - \underline{P}_n(t+\delta t)\right| = \frac{(t_2 - t - \delta t)w_1}{(t_2 - t_1)} \quad \text{(A9)}$$

and substituting for $\underline{P}_n(t+*t)$ from Equation A8, Equation A9 may be rewritten as

$$\left|p(t)\underline{A} + \underline{B}\right| = \frac{(t_2 - t - \delta t)w_1}{(t_2 - t_1)}, \quad \text{(A10)}$$

where

$$\underline{A} = -\frac{(t_2 - t_1)\delta t}{w_1(t_2 - t)}\left(\underline{P}_v(t) - \underline{P}_n(t)\right) \quad \text{(A11)}$$

and

$$\underline{B} = \underline{P}_v(t+\delta t) - \underline{P}_n(t) - \delta t\underline{C}\left(z_n(t)\right). \quad \text{(A12)}$$

Expanding Equation A10, we get the quadratic equation

$$\underline{A} \bullet \underline{A}p(t)^2 + 2\underline{A} \bullet \underline{B}p(t) + \underline{B} \bullet \underline{B} = \left[\frac{(t_2 - t - \delta t)w_1}{(t_2 - t_1)}\right]^2, \quad \text{(A13)}$$

which may be solved for $p(t)$ in the usual manner.

In solving Equation A13, the solution using the positive square root was ignored because it led to large values of $p(t)$ and large vertical oscillations in the net path.

Flow of water through the net

Because, by assumption 4 above, the net mouth was always perpendicular to the warp, the flow of water through the net at time t (in m3/s) is given by

$$F(t) = 2\underline{V}_{nw} \bullet \underline{U}_{wp}, \quad \text{(A14)}$$

where V_{nw} is the velocity of the net relative to the water, given approximately by

$$\underline{V}_{nw} = \frac{\underline{P}_n(t+\delta t) - \underline{P}_n(t)}{\delta t} - \underline{C}\left(z_n(t)\right), \quad \text{(A15)}$$

$\underline{U}_{wp}$ is a unit vector in the direction of the warp, given by

$$\underline{U}_{wp} = \frac{\underline{P}_v(t) - \underline{P}_n(t)}{\left|\underline{P}_v(t) - \underline{P}_n(t)\right|}, \quad \text{(A16)}$$

and factor 2 is the net mouth area in m^2.

Calculation of correction factors

The correction factor associated with a horizontal layer of water is given by

$$CF = \frac{\textit{Thickness of layer}}{\textit{Volume of water filtered by net within layer}}. \quad \text{(A17)}$$

Thus, for the layer of water that the net passed through between times t and t+*t, the correction factor is given approximately by

$$\frac{z_n(t) - z_n(t+\delta t)}{F(t)\delta t}.$$

which is treated as the correction factor associated with depth $z_n(t)$. Thus, for each plankton tow, correction factors for depths $z_n(t_1)$ (=z_{n1}), $z_n(t_1$+*$t)$, $z_n(t_1$+2*$t)$, etc. were calculated.

Finally, the correction factor for a given egg stage at a given plankton tow was calculated, by interpolation, as the correction factor at the mid-point of the depth layer associated with that egg stage.

Appendix 2: Calculation of centroids

This appendix describes the procedure for calculating the centroid (= center of gravity) of each age group (plotted in

Fig. 4A). First, the survey area was divided into 36 subareas (Fig. 4A). The longitude of the centroid for age group a, X_a, was estimated by using

$$X_a = \frac{\Sigma_j x_j M_{aj} A_j}{\Sigma_j M_{aj} A_j},$$

where $M_{aj} = \frac{1}{n_j}\Sigma_j C_{aij}$

and C_{aij} = catch rate (eggs/m^2) for age group a at the ith station in subarea j;
M_{aj} = mean catch rate for age group a in subarea j;
n_j = number of stations in subarea j;
A_j = area of subarea j; and
x_j = longitude of center of subarea j.

The latitudes of the centroids were calculated similarly. These calculations use the approximation that, for each age group, the centroid of eggs within a subarea is at the center of the subarea.

Appendix 3: Egg production model and estimation

This appendix describes the calculation of daily egg production, N_0, and CV given in Table 4 and shown in Figure 6. It is assumed that

1 the rate of egg production was constant (both from day to day and within each day) in the period immediately preceding and during the plankton survey,
2 egg mortality was constant over the same period and independent of age, and
3 the egg abundance estimates, N_a, of Table 3 are unbiased and lognormally distributed with CV's, c_a, as given in Table 3.

Under these assumptions, E_a, the expected value of N_a, is given by

$$E_a = \int_{t_{a-1}}^{t_a} N_0 e^{-zt} dt = \frac{N_0}{Z}\left(e^{-Zt_{a-1}} - e^{-Zt_a}\right),$$

where N_0 = the daily egg production (eggs/day);
Z = the daily instantaneous egg mortality (per day); and
(t_{a-1}, t_a) = the range of ages (day) in age group a.

The mean age of eggs of age group a (used in Fig. 6) is given by

$$\frac{1}{E_a}\int_{t_{a-1}}^{t_a} tN_0 e^{-Zt} dt = \frac{1}{Z} + \frac{\left(t_a e^{-Zt_a} - t_{a-1}e^{-Zt_{a-1}}\right)}{e^{-Zt_a} - e^{-Zt_{a-1}}}.$$

N_0 and Z were estimated by maximum likelihood, ie. by maximizing the likelihood, L, which is given by (ignoring constants)

$$L = \prod_a \left[\frac{1}{N_a}\exp\left(-0.5\sum_a\left[\frac{1}{\sigma_a}\log\left(\frac{N_a}{E_a}\right) + 0.5\sigma_a\right]^2\right)\right],$$

where σ_a is the standard error of $\log(N_a)$, given by

$$\sigma_a = \left[\log(1+c_a^2)\right]^{\frac{1}{2}}.$$

By definition, Z must be positive. However, in the bootstrap procedure described next, it sometimes happened that the maximum likelihood estimate of Z was negative (because, by chance, simulated egg abundance estimates increased with age). When this happened, Z was forced to be zero, so that

$$E_a = N_0(t_a - t_{a-1}).$$

The following bootstrap procedure was used to estimate the degree of uncertainty in the estimates of N_0 and Z.

1 the maximum likelihood estimates of N_0 and Z were used to calculate the expected egg abundances, E_a, using the formula above;
2 new egg abundance estimates, N_a, were simulated by using lognormal distributions with expected values, E_a, and CV's, c_a;
3 maximum likelihood estimates of N_0 and Z were calculated from the simulated values of N_a, and
4 steps 2 and 3 were repeated 1,000 times.

The resulting 1,000 values of N_0 and Z are the bootstrap distributions for these parameters; the 0.025 and 0.975 quantiles of these distributions were taken as bounding the 95% confidence intervals for each parameter. The CV's of these distributions are taken as estimates of the CV's of the maximum likelihood estimates of N_0 and Z.

Appendix 4: Analysis of ovarian samples

Ovaries frozen onboard were thawed in the laboratory, weighed, and then one of the two slit open. A subsample of about 5 g was scraped from the full length of one ovary from each fish, because preliminary analyses had indicated there was some variation in egg density from different parts of the ovary. The subsample was then placed into 1M KOH for a period of 5–15 minutes depending on the ovarian stage. Maturing oocytes (stage 3) were bound more tightly in the matrix than advanced stages, and therefore needed a longer KOH treatment to separate individual oocytes. Stage-3 oocytes generally retained a medium orange color after KOH treatment, and thus needed no further treatment after separation. However, the more transparent stage-4, stage-5, and stage-8 oocytes were stained with Semichon's carmine. The subsample was then washed through a 0.7-mm mesh sieve that was found to be of a suitable mesh size to retain oocytes with a diameter greater than about 1.2 mm. Primary, early vitellogenic, and atretic oocytes, as well as small fragments of matrix and tissue

passed through the mesh. Atretic eggs, in particular, had dimensions of 0.5 to 1.0 mm (from histological observations) and were found to wash through the sieve. The mean size of stage-3 oocytes was 1.56 mm (range 1.30–1.83 mm, SE=0.01). More advanced stages had larger oocytes (stage 4=2.15 mm; stage 5= 2.55 mm; stage 8=2.20 mm) and therefore were fully retained.

Eggs were then counted with an electronic egg counter incorporating a phototransistor (Bycroft, 1986). Eggs were siphoned from a large beaker into a perspex chamber with a vacuum pump attached to the top of the chamber. Water flow was regulated to keep this chamber about three-quarters full, so that any air bubbles rose to the top. Eggs passed from the bottom of the chamber through a small tube past a phototransistor and light source. The reduction in light intensity (caused by the presence of the eggs) was detected by the phototransistor and was recorded on an electronic counter with digital readout. The rate of flow was regulated to avoid large numbers of eggs in the chamber and exit tube at any one time (which could result in multiple eggs passing the counter at the same time and being recorded as only as one egg). A gain control (set very low) was used to alter the sensitivity of the counter so that small fragments of extraneous material that remained after the sieving were not counted.

Checks of the accuracy of the electronic counter were made by comparing manual counts (made with a dissecting microscope) with electronic counts and no significant difference was found (t-test, $P<0.01$, number of comparisons=4). Also, a reference set of a known number of eggs was regularly used to check the calibration. Up to four determinations were made in each trial, which produced CV's of the mean count of generally less than 0.01.

Total fecundity from both ovaries was initially calculated from the number of oocytes/g × ovarian weight. Although this is common practice in fecundity studies, it may introduce bias because ovary weight includes ovary wall which does not contain eggs. Several comparisons were made between estimated fecundity based on the scaled-up subsample count, and actual counts of all oocytes in an ovary. Scaled-up subsample counts typically overestimated actual fecundity by 10–20%. The proportion of wall weight to total ovary weight (for stages 3, 4, 5, and 8) were estimated by stripping a number of weighed ovaries of all eggs and weighing the remaining wall (Appendix 4, Table 1). The proportions were then used to adjust the total fecundities of each fish in each stage. The higher proportions for stages 5 and 8 are to be expected because some stage-5 fish may be in the act of spawning and stage-8 fish have already spawned some of their eggs; therefore the ovary wall is a greater proportion of total ovary weight.

Table 1

The contribution (percentage) of the ovary wall to ovary weight at each ovarian stage. See text for stage definitions.

Stage	Mean	SE	*n*
3	9.6	1.2	15
4	6.6	0.4	14
5	13.9	2.7	14
8	29.7	4.4	19